Pharmaceutical Research, Vol. 24, No. 1, January 2007 (© 2006)
DOI: 10.1007/s11095-006-9128-9

Research Paper

Aqueous-Soluble, Non-Reversible Lipid Conjugate of Salmon Calcitonin: Synthesis, Characterization and *In Vivo* Activity

Weiqiang Cheng,[1] Seetharama Satyanarayanajois,[2] and Lee-Yong Lim[3,4]

Received April 28, 2006; accepted July 18, 2006; published online November 16, 2006

Purpose. A novel, non-reversible, aqueous-based lipidization strategy with palmitic acid as a model lipid was evaluated for conjugation with salmon calcitonin (sCT).
Materials and Methods. A water-soluble ε-maleimido lysine derivative of palmitic acid was synthesized from reaction of palmitic acid *N*-succinimidyl ester and ε-maleimido lysine. The latter was generated from reaction of α-Boc-lysine and methylpyrrolecarboxylate, with subsequent deprotection of the Boc group. The palmitic derivative was further conjugated with sCT via a thio-ether bond to produce Mal-sCT in aqueous solution. The identity and purity of Mal-sCT was confirmed by Electrospray Ionisation Mass spectrometry (ESI–MS) and HPLC.
Results. Yield of Mal-sCT was 83%. Dynamic light scattering and circular dichroism data suggested that Mal-sCT presented as a stable helical structure in aqueous solutions of varying polarity, with a propensity to aggregate at concentrations above 11 μM. Cellular uptake of Mal-sCT was twice that of sCT in the Caco-2 cell model, and the conjugate was more resistant to liver enzyme degradation. Mal-sCT exhibited comparable hypocalcemic activity to sCT when administered subcutaneously in the rat model at sCT equivalent dose of 0.114 mg/kg. Peroral Mal-sCT, however, produced variability in therapeutic outcome. While four out of six rats did not respond following intragastric gavage with Mal-sCT, two rats showed significantly suppressed plasma calcium levels (~60% of baseline) for up to 10 h.
Conclusion. A novel non-reversible, water-soluble lipid conjugate of sCT was successfully synthesized that showed (1) different aggregation behavior and secondary structure, (2) improved enzymatic stability and cellular uptake, and (3) comparable hypocalcemic activity *in vivo* compared to sCT.

KEY WORDS: activity; conjugation; lipidization; oral delivery; salmon calcitonin; synthesis.

INTRODUCTION

Lipid conjugation is a promising method for increasing the deliverability of a peptide drug. The lipid can facilitate interaction between the peptide and its binding sites on the cell membrane, and promote a depot effect through binding to plasma proteins and the local administration site (1,2). Lipid modification can also increase the enzymatic stability of the peptide drug (3,4). Collectively, these properties may contribute towards delayed systemic absorption and increased plasma circulation time, which can lead to prolonged or even enhanced efficacy. This is seen with insulin detemir [NN-304, also known as Lys B29-tetradecanoyl des-(B30) human insulin], a soluble, long-acting insulin which shows a flat time–action profile over 12 h and a long clearance rate from its subcutaneous injection site (5). Likewise, stearoyl acylated antiviral antibodies have been observed to suppress virus reproduction by 100-fold greater than non-modified antibodies because of their capacity for intracellular penetration (6).

Despite its potential, lipidization frequently results in reduced or, in some cases, loss of bioactivity of a pharmaceutical (7,8). To confer the benefits of lipidization without sacrificing efficacy, Shen's group designed a novel method, known as reversible aqueous lipidization (REAL), in which water-soluble lipid groups were conjugated to a peptide drug via inter-disulfide bonds (9–12). This method has been shown to be particularly useful for potentiating the activity of peptide drugs with an intra-disulfide bond, such as desmopressin (10,11), calcitonin (12) and octreotide (13). The potentiated activities appeared to be related to the enhanced stability of the conjugates and their capacity to bind to local tissues and plasma proteins. For these reversible conjugates, activity *in vivo* was associated with the regeneration of the parent drug after oral or subcutaneous administration. There was evidence, however, that the REAL–peptide conjugate itself might be active (12).

[1] Department of Pharmacy, National University of Singapore, 18 Science Drive 4, Singapore, 117543, Singapore.
[2] Department of Basic Pharmaceutical Sciences, University of Louisiana, 700 University Avenue, Monroe, Louisiana 71209, USA.
[3] Pharmacy, School of Biomedical, Biomolecular and Chemical Sciences, University of Western Australia, 35 Stirling Highway, Crawley, Washington 6009, Australia.
[4] To whom correspondence should be addressed. (e-mail: limly@cyllene.uwa.edu.au)

ABBREVIATIONS: APCI, Atmospheric Pressure Chemical Ionization; BA, Bioavailability; ESI, Electrospray Ionisation; MS, Mass spectrometry; TCEP, tris(2-carboxyethyl)phosphine; sCT, salmon calcitonin.

On that basis, we examined the structure–activity relationships of peptide drugs with intra-disulfide bonds, and found further evidence that the intra-disulfide bond is frequently not essential for activity. For example, the replacement of the disulfide moiety in desmopressin with a sulfide–methylene group resulted in a longer duration of activity (14). An analogue of octreotide, PTR 3173, which did not have an intra-disulfide bond, was shown to be as potent as octreotide in inhibiting forskolin-stimulated cAMP accumulation in several cell lines (15,16). Linear salmon calcitonin (sCT) analogues without an intra-disulfide bond also possessed intact hypocalcemic activity in the rat model (17). More recently, the sCT *S*-sulfonated analog was shown to have a more potent activity than sCT in rats (18). These findings led us to hypothesize that the disulfide bond in peptide drugs might be a potential site for non-reversible lipidization. The argument for non-reversible lipidization is that it maintains greater conjugate stability, and therefore greater assurance of realizing the lipid-mediated advantages *in vivo* compared to a labile lipid conjugate.

To date, there is no report on a non-reversible aqueous-based lipid modification method targeted at the intra-disulfide bond of a peptide drug. In this paper, we describe a novel non-reversible, aqueous-based lipid conjugation method targeted at the intra-disulfide bond of salmon calcitonin, a model drug. This method is unique compared to other non-reversible lipidization methods (19–21) because it utilizes an aqueous medium, which is environmentally friendlier than noxious organic solvents, and gives very high yield. It may therefore be a useful generic tool for the lipidization of peptide drugs with sulfide–ether bonds.

MATERIALS AND METHODS

Materials

Salmon calcitonin (sCT) was purchased from Unigene Laboratory (Boonton, NJ, USA). *N*-α-(*tert*-butoxycarbonyl)-l-lysine (*N*-Boc-lysine), Hanks Balanced Salt Solution (HBSS), *N*-2-hydroxyethylpiperazine-*N*′-2-ethanesulfonic acid (HEPES), trifluoroethanol, methylpyrrolecarboxylate, palmitic acid *N*-succinimidyl ester (Pal-Suc), tris(2-carboxyethyl) phosphine (TCEP), trifluoroacetic acid (TFA), fluorescein-5-isothiocyanate (FITC) and calcium standard solution (1.000 mg/ml) were from Sigma-Aldrich (St. Louis, MO, USA). Minimum essential medium (MEM) and fetal bovine serum (FBS) were from Gibco BRL Life Technology (Grand Island, NY, USA). Acetonitrile and isopropanol of HPLC grade were from Fisher Scientific (Irvine, CA, USA), and Milli-Q water was used for HPLC mobile phase.

Finnegan MAT LCQ mass spectrometer, equipped with an Electrospray Ionization (ESI) or Atmospheric Pressure Chemical Ionization (APCI) source, and coupled with Xcalibur LCQ Tune Plus Version 1.0 SR software (San Jose, CA, USA), was used for mass spectrometry analysis. The MS spectrometer settings were as follows: capillary temperature 270°C; shealth gas 75 unit/min; auxiliary gas 20 unit/min, spray voltage 4 kV, capillary voltage 10 V. LC flow rate: 0.5 ml/min (50% methanol). Injection volume: 20 µl. Bruker 300 M NMR was used for all the NMR analyses.

Synthesis of Water-Soluble Palmitic Acid Derivative

N-ε-*Maleimido* α-*Boc*-L-*Lysine*

N-ε-maleimido α-Boc-L-lysine (II) was synthesized according to published methods (22,23) with slight modification, as shown in Fig. 1A. Briefly, 1.56 g (10 mmol) of methylpyrrolecarboxylate and 2.46 g (10 mmol) of *N*-Boc-l-lysine (I) were mixed in saturated aqueous $NaHCO_3$ at 0°C for 2 h. The solution was acidified to pH 3 with 20% of H_2SO_4 before extraction with ethyl acetate. The organic layers were combined and the residue after solvent evaporation was isolated by silica-gel column flushing with chloroform–methanol stepwise gradient. The target was pooled together and solvent was evaporated. This reaction resulted in 2.70 g of *N*-ε-maleimido α-Boc-L-lysine (II) (yield 84.5%).

^{1}H-NMR ($CDCl_3$) δ ppm: 1.30–1.95 (6H, m, $(CH_2)_3$), 1.44 (9H, s, Boc($COCCH_3)_3$), 3.52 (2H, t, NCH_2), 4.28 (1H, m, α-CH), 5.08 (1H, d, -NHCO-), 6.69 (2H, s, maleimido-H). ESI–MS (MNa^+): *m*/*z* 348.3 (calculated 349.3). ^{13}C-NMR ($CDCl_3$) δ ppm: 22.5 (lysine-γ-CH_2), 27.8 (lysine-β-CH_2), 28.1 (Boc-CH_3), 31.6 (lysine-δ-CH_2), 37.2 (lysine-ε-CH_2), 52.9 (31.6 (lysine-α-CH_2), 81.5 (Boc-C-), 133.9 (maleimido-CH), 155.5 (Boc-CO-), 170.7 (maleimide-CO-), 176.2 (lysine-COOH).

ε-Maleimido Lysine Derivative of Palmitic Acid (Pal-Lys-Mal)

Pal-Lys-Mal (IV) was synthesized based on a previous report (23) with slight modification. *N*-ε-maleimido α-Boc-L-lysine (II) (0.8104 g, 0.24 mmol) was reacted with 8 ml of saturated HCl in dry ethyl acetate (prepared by flushing dry HCl with ethyl acetate) for 30 min at room temperature before addition of 3 ml of dry ether at 0°C. HCl salt of *N*-ε-maleimido-L-lysine (III) (0.4675 g, 1.78 mmol, 71.6% yield) was isolated by precipitation and filtration.

N-ε-maleimido-L-lysine HCl (III) (0.47 g, 1.78 mmol) was added without further purification to 0.71 g (2.02 mmol) of Pal-Suc and 493 µl (3.56 mmol) of triethyl amine in 15 ml of dimethylformide (DMF). The reaction mixture was stirred at room temperature for 0.5 h, then diluted with 100 ml of water. The precipitate was collected via filtration and dried *in vacuo*. The residue was eluted in a silica gel column using a mixture of chloroform, methanol and acetic acid (100:2:0.01) as eluent to produce the target Pal-Lys-Mal (IV) (0.282 g, 34.2% yield).

APCI–MS (MH^+): experimental m/z: 465.0 (calculated: 465.6). ^{1}H-NMR ($CDCl_3$) δ ppm: 0.84 (3H, CH_3), 1.22 (26H, m, $(CH_2)_{13}$), 1.58 (4H, m, lysine-γ,δ- CH_2), 1.70-1.94(2H, m, lysine-β-CH_2), 2.23 (2H, t, $COCH_2$), 3.48 (3H, t, CH_3), 4.51 (1H, q, lysine-α-CH), 6.46 (1H, d, CONH), 6.67 (2H, d, maleimido-H), 9.33 (1H, broad, COOH). ^{13}C-NMR ($CDCl_3$) δ ppm: 174.91, 174.33, 170.85, 134.02, 52.06, 37.14, 36.32, 31.81, 31.16, 29.60, 29.57, 29.55, 29.43, 29.24, 29.18, 27.94, 25.57, 22.57, 22.22, 13.99.

Conjugation of Pal-Lys-Mal with sCT

Conjugation of Pal-Lys-Mal with sCT generated the conjugate, Mal-sCT (V), as shown in Fig. 1A. Mal-sCT was prepared by mixing, with stirring, 31.12 mg of sCT and 27.0 mg of

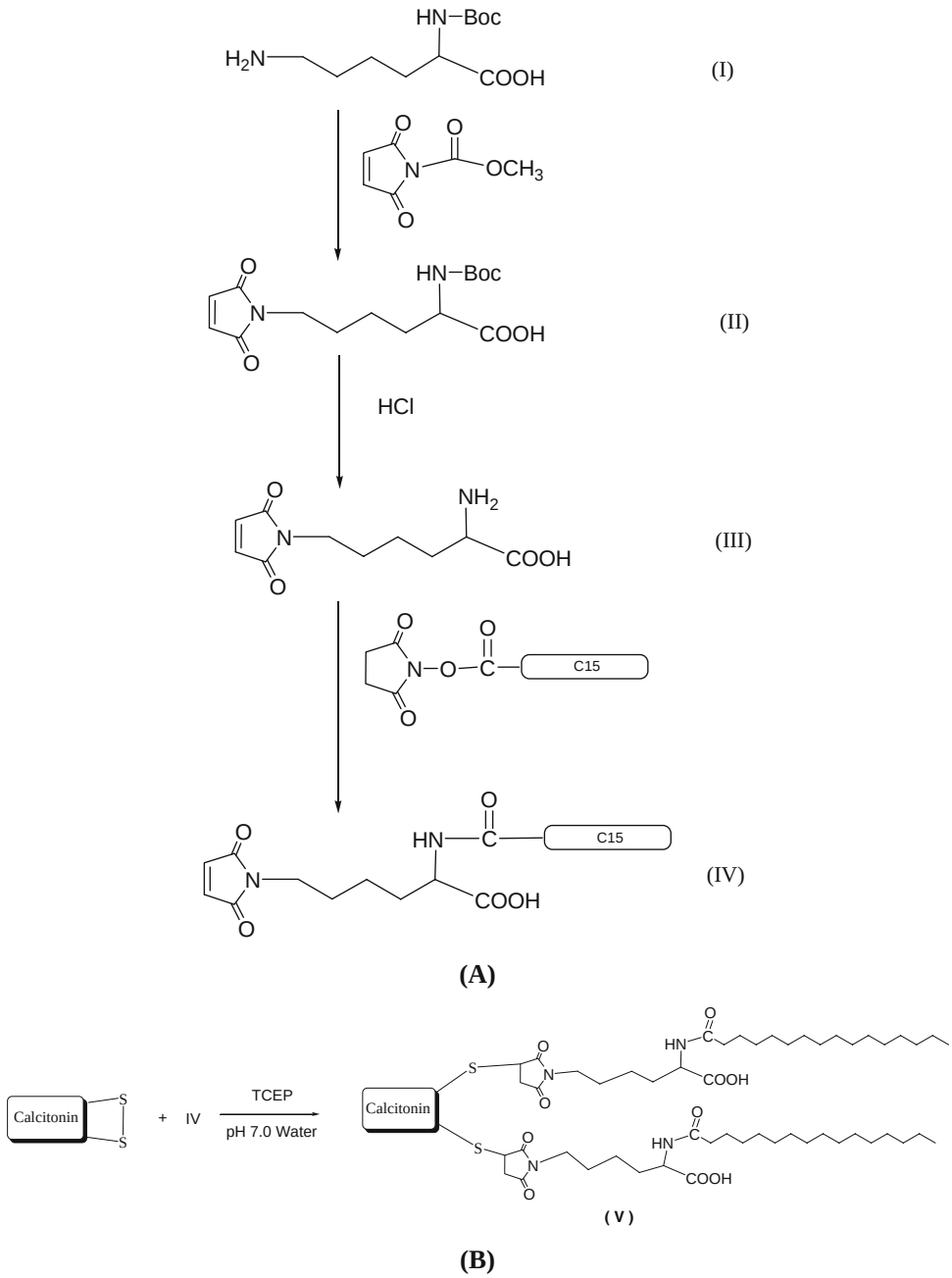

Fig. 1. Schematic diagram showing the synthesis pathway of (A) ε-Maleimido Lysine Derivative of Palmitic acid (*Pal-Lys-Mal*, IV) and (B) conjugation of Pal-Lys-Mal to sCT.

Pal-Lys-Mal (IV), together with 30 mg of tris(2-carboxyethyl)-phosphine (TCEP), in 0.5 M of pH 7.0 phosphate buffer under argon protection at 0°C for about 20 h.

Mal-sCT was separated from the reaction mixture in a C-18 semi-preparative column (10×250 mm) with the elution system: A: 0.1% TFA in water and B: isopropanol and acetonitrile (1:1 v/v) mixture containing 0.1% TFA; from 50% B to 90% B in 40 min at a flow rate of 2 ml/min. The fractions containing the target were collected and pooled together, and after the evaporation of the organic solvent in a rotary evaporator, the concentrated target was lyophilized and identified with ESI–MS by comparing the experimental and calculated m/z values based on an exact mass of 4,360.4 Dalton for MW of Mal-sCT.

The purity of Mal-sCT was confirmed with HPLC. HPLC analysis was carried out using a Waters Symmetry300 C-18 column (4.6×250 mm). Elution time profile was from 100% A: water (0.1% TFA) to 100% B: 1:1 v/v mixture of isopropanol and acetonitrile (0.1% TFA) in 40 min and maintaining at 100% B for another 5 min. Volume of sample injected was 100 μl and the sample was detected at λ=214 nm.

Circular Dichroism

CD spectra were obtained with a Jasco J810 spectrophotometer instrument.Spectra were acquired over a wavelength range of 190 to 260 nm. The N_2 flow rate was set at 5 l/min.

The sample cuvette (200 μl) was cleaned until blank samples (0, 20, and 50% of trifluoroethanol (TFE) in water) showed optical density of less than 0.5 mDeg. The spectra of test samples, which comprised of 0.10 mM of sCT or Mal-sCT in distilled water or aqueous TFE solutions (0–50%), were recorded with the corresponding solvents serving as blanks.

Dynamic Light Scattering (DLS)

Data collection was performed using the ProteinSolutions DynaPro Dynamic Light Scattering Instrument at a laser wavelength of 825.8 nm, detection angle of 90°, and typical sample volume of 20 μl. Each light scattering experiment consisted of 20 or more independent readings, and the data were analyzed using the DynaPro Instrument Control Software for Molecular Research DYNAMICS (version 5.26.60). Samples were dissolved in distilled water at 2.50, 11.2, 50.0, 220 and 1,000 μM concentrations. To minimize dust interference, all solutions were freshly prepared and centrifuged at 2,000 rpm for 2 min (Eppendorf centrifuge 5417, Hamburg, Germany) immediately prior to analysis. Particle size data are presented as mean ± polydispersity.

Stability to Intestinal Metabolism

The protocol for studying peptide stability in intestinal fluid was adapted with modifications from a published report (24). Rats (n=3) were fasted for 24 h before they were euthanized by IP injection of ketamine (150 mg/kg) and xylazine (20 mg/kg). An abdominal incision was made to expose the intestine, and 30–40 cm of small intestine, starting from the duodenum, was excised from each rat. The lumen of each intestinal segment was immediately flushed with 7.5–9.0 ml of ice-cold PBS buffer (pH 6.6). The washings from all the intestinal segments were pooled, and the protein content (1.2~1.5 mg/ml) was determined using the MicroBCA assay, with bovine serum albumin as standard. The degradation experiments were initiated by incubating 40 μM of sCT or Mal-sCT with intestinal fluids at a final intestinal protein concentration of 45 μg/ml. The mixtures were shaken at 50 rpm in a water bath at 37°C. At specific time points, 150 μl aliquot of the incubation mixture was withdrawn and the enzyme reaction was quenched by adding 10 μl of acetic acid. The amount of sCT or Mal-sCT remaining was determined by HPLC assay as described above.

Stability to Liver Metabolism

A previously described *in vitro* metabolic system (11) was adopted with slight modification to investigate the enzymatic stability of sCT and Mal-sCT. A fresh liver (7.5 g), harvested from a euthanized normal Wistar female rat (240 g), was soaked in normal saline, then triturated and mixed with 7.5 ml of MEM solution containing 5% FBS. The mixture was centrifuged at 2,000 rpm at 4°C (Hettich Zentrifugen, Tuttlingen, Germany) for about 2 min, and the supernatant was collected. Lyophilized sCT and Mal-sCT were separately added to aliquots of the supernatant to give final concentration of 0.1 mM, and the mixtures were incubated in a water bath operating at 37°C and a shaking frequency of 60 rpm. The reacting mixtures were sampled at 0, 15, 30, 45, 60, 90, and 120 min. Ethanol (125 μl) was immediately added, under vortex, to each withdrawn sample (50 μl) to quench the reaction, and the supernatant fractions (120 μl), isolated by centrifugation of the samples, were analyzed by HPLC as described above.

Uptake by Caco-2 Cells

sCT and Mal-sCT were labeled with the fluorophore, FITC, to allow for their quantification in cellular uptake experiments. Synthesis of FITC-sCT and FITC-Mal-sCT was based on the reaction between the isothiocyanate group of FITC and the primary amino groups of lysine and N-terminal amine in the peptides (25). The conjugation reaction, at a drug to FITC molar ratio of 1:2, was carried out in pH 9.0 $NaHCO_3$ solution at 0–4°C for 3 h. The reactions were quenched by adding 5 ml of pH 4.0 ammonium acetate solutions. Fractions containing the FITC-labeled peptides were isolated by elution in a semi-preparative HPLC column and lyophilized. The labeling efficiency was determined by calculating the relative peak heights of unlabeled and labeled drugs obtained from MS measurements. Labeling efficiencies for 1 FITC- and 2 FITC-labeled sCT were 56.9 and 7.1%, respectively. Corresponding labeling efficiencies for Mal-sCT were 37.1 and 4.9%.

Cellular uptake experiments were conducted according to the established protocols in our laboratory (26). Freeze-dried FITC-labeled samples were dissolved in the uptake medium (HBSS containing 10 mM HEPES and buffered to pH 7.4) to give 5.0 μM sCT or Mal-sCT solution. Caco-2 cells (passage 56, American Type Culture Collection, Rockville, MD) were cultured for 10 days on 96-well polycarbonate plates (NuncTM, Nalge Nunc International, Denmark) at a seeding density of 2×10^4 cells/well. The cells were washed thrice with pre-warmed uptake medium and equilibrated for 1 h with 100 μl of the medium at 37°C. After the uptake medium was aspirated, the cells were incubated with 100 μl of test samples for up to 145 min at 37°C. The experiments were terminated by aspirating the test samples and washing the cells three times with ice-cold PBS. To each well was added 100 μl of uptake medium, and the cells were solubilized 1 h later with 100 μl/well of 0.2 M NaOH/0.5% Triton-100. The cell lysates were measured for fluorescence using a plate reader (Spectra Fluor, Tecan Group Ltd., Männedorf, Switzerland; λexc 485 nm, λemi 535 nm) calibrated with FITC-sCT and FITC-Mal-sCT samples (0.05 to 2.5 μM) dissolved in 1:1 v/v of uptake medium and the lysate of control cells. Cell-associated FITC-sCT and FITC-Mal-sCT was expressed as a percent of the initial amount administered to each well (mean ± SD, n=6).

Pharmacodynamic Response

Pharmacodynamic response of the conjugates was evaluated by analysis of plasma calcium concentration and the area above the intensity curve (AAIC) in the rat model (27). Wistar female rats weighing 170 ~ 220 g (about 8 weeks old) were purchased from the National University of Singapore (NUS) Centre for Animal Resources, and housed at the NUS Animal Holding Unit. All experimental protocols involving animals were approved by the Animals Ethics Committee of

NUS. The rats were divided randomly into groups of six after 3 days of acclimatization, and the pharmacodynamic response was assessed following subcutaneous and oral administration of sCT and Mal-sCT.

For subcutaneous administration, sCT and Mal-sCT were separately dissolved in normal saline at 0.114 and 0.145 mg/ml, respectively, and injected under the dorsal skin of the rat using a 27-gauge needle. The dose for Mal-sCT was calculated to give equimolar concentration as the dose for sCT. For oral administration, sCT and Mal-sCT were dissolved in distilled water to prepare 2.5 mg/ml sCT equivalent solutions. The rats were fasted for 12–16 h before they were administered by intragastric gavage via an 18-gauge gavage needle with 5.0 mg/kg of sCT or 6.4 mg/kg of Mal-sCT (equivalent to 5.0 mg/kg sCT). Control rats were administered with normal saline. Immediately before, and at 1, 2, 4, 8, 12, 18, 24 h after administration of sCT or Mal-sCT, blood samples (120–150 μl) were collected by saphenous vein puncture with a Microvette® CB300LH (Sarstedt, Germany). Blood plasma was obtained by centrifuging the samples at 5,000 rpm (Eppendorf Centrifuge 5145D) for 10 min at 15°C.

Plasma calcium level was assayed by atomic absorption spectrometry (Perkin Elmer AAnalyst 100, MA, US) using a hollow calcium lamp at λ=422.7 Å as the light source (28). Slit width was 0.7 nm and pure ethyne /compressed air flame was used. Calibration was performed using standard solutions that contained 5.0, 10.0 and 15.0 mg/dl of calcium, together with 140 mM of NaCl and 5 mM of KCl. Blank solutions comprised of 140 mM of NaCl and 5 mM of KCl without calcium. The standard and blank solutions, as well as all plasma samples, were diluted 50-fold with a solution containing 10 mM of $LaCl_3$ and 37 mM of HCl before they were analyzed. Average recovery of calcium using this method was 100.3% (RSD=3.8%, n=3) over the concentration range of 5.55 to 13.3 mg/dl.

Plasma calcium *versus* time graphs were constructed, and the linear trapezoidal method was applied to determine the AAIC. Relative pharmacological bioavailability, F, was calculated according to Eq. 1:

$$F = \frac{\mathrm{AAIC}(oral)}{D(oral)} \div \frac{E\max}{D\min/\max} \quad (1)$$

where AAIC referred to the area above the plasma calcium–time curve, D was the dose administered, Dmin/max was the minimum dose required for maximum calcium lowering effect, and Emax was the hypocalcaemic activity at this dose. Emax and Dmin/max for subcutaneously administered sCT had the values of 426.8 mg min/dL and 10.2 ng/rat (100–250 g), respectively (27). Since the absolute bioavailability of sCT following subcutaneous injection was 16.1% on a rat model (27), the absolute pharmacological bioavailability for the orally administered peptides was calculated as $F\times16.1\%$.

Statistical Analyses

Results are expressed as mean ± standard deviation. Plasma calcium and cellular uptake data were analyzed by one-way ANOVA, with post-hoc Tukey's tests and Independent-Sample t-test applied, respectively, for the comparison of group means at a p value of 0.05 (SPSS 12.0, SPSS Inc., Chicago, IL).

RESULTS

Synthesis of Mal-sCT

The synthesis pathways for the water-soluble lipid, Pal-Lys-Mal (IV), and the subsequent conjugation of sCT with Pal-Lys-Mal are shown in Fig. 1. Pal-Lys-Mal was synthesized by palmitoylation of ε-maleimido-lysine (III) with Pal-Suc.

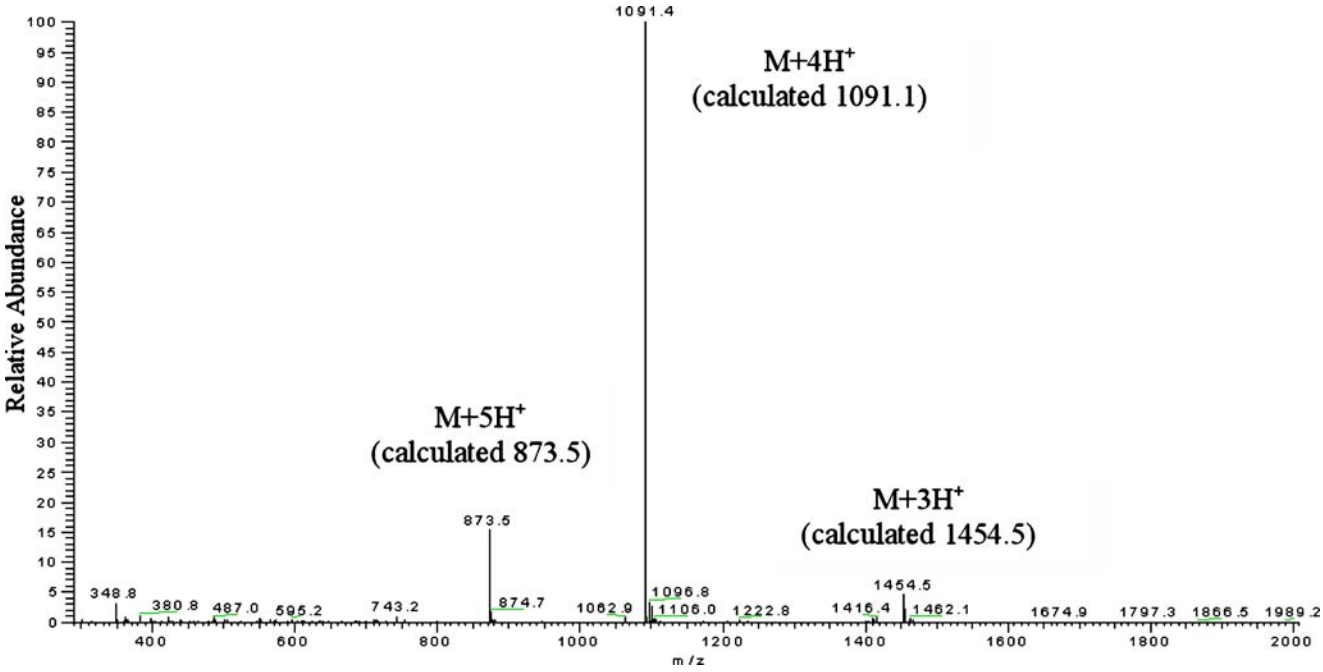

Fig. 2. Mass spectrum of purified Mal-sCT in water.

ε-maleimido-lysine was obtained by de-protection of ε-maleimido α-Boc lysine (II), which was derived by attaching a maleimido group at the ε-amine of α-Boc-lysine via an imide–amide intermediate (22). The presence of the maleimido groups was readily confirmed by ^{1}H-NMR (single peak 6.70 ppm) and ^{13}C-NMR (134 ppm) spectra.

Conjugation of Pal-Lys-Mal with sCT was conducted by one-pot synthesis (Fig. 1B). The intra-disulfide bond of sCT was reduced by TCEP to form thiols in an aqueous environment at pH 7.0 and, without separation, further reacted with the maleimido group of the lipid to yield the thiol-ether bond of Mal-sCT. Despite the mild conditions of synthesis, the conjugation process was very efficient, giving a high yield (83%) of the purified conjugate.

The ESI–MS spectrum (Fig. 2) of the conjugate showed an array of main peaks at 873.5 (17%), 1,091.4 (100%) and 1,454.5 (7%), which agreed well with the calculated m/z values for Mal-sCT: 873.1($M+5H^+$), 1,091.1($M+4H^+$) and 1,454.5 ($M+3H^+$), respectively. HPLC analysis (Fig. 3) of the conjugate suggested a pure single compound with higher lipophilicity than sCT.

Circular Dichroism Spectra

The CD spectrum of sCT in water showed no apparent secondary structure (Fig. 4A). Upon the addition of TFE, an organic solvent with low dielectric constant, sCT showed a positive peak at 192 nm and two negative peaks at 208 nm and 222 nm, respectively, suggesting the presence of a helical structure. This structure became more evident at higher TFE concentrations. In contrast, the Mal-sCT exhibited comparable CD spectra whether it was dissolved in water or in aqueous solutions of TFE (Fig. 4B). The CD spectra of Mal-sCT suggest a helical structure for the conjugate that was stable and less dependent on the environment than that for sCT.

Size Measurements

Figure 5 shows the mean particle size measured by dynamic light scattering analyses of sCT and Mal-sCT in distilled water. sCT (MW 3.43 kDa) had mean radii of 1.1 nm in the concentration range of 220 to 1,000 μM, which translated to a calculated MW of 4.69 kDa, comparable with the MW of sCT. This suggests that sCT in distilled water existed mainly as monomers. Further dilution of the sCT solution resulted in very low photon counts (results not shown), making it difficult to take measurements against the background noise. As the dilution of sCT was not likely to cause peptide fragmentation, the implication is that the particle size of sCT could not be accurately measured below a critical concentration. By comparison, Mal-sCT (MW 4.36 kDa) had radii of 3.1 to 3.6 nm over a wide concentration range of 11.2 to 1,000 μM. The particle size range was equivalent to a calculated MW of between 46.02 and 66.37 kDa. Further dilution of the Mal-sCT solution to 2.5 μM resulted in a hydrodynamic radii of 1.3 nm, equivalent to 6.38 kDa, or 1.5 times the MW of Mal-sCT. These data suggest that Mal-sCT in aqueous solutions might have transited from aggregated to monomeric states when diluted from 11.2 to 2.5 μM.

Intestinal Metabolism

Figure 6 shows the degradation profiles of sCT and Mal-sCT in the diluted intestinal solutions. Degradation of sCT was almost complete within 5 min, the degradation data fitting well with the first order kinetics ($Y=100e^{-1.20X}$ and $R^2=0.96$). Degradation of Mal-sCT was less well defined by first order kinetics ($Y=100e^{-0.043X}$, $R^2=0.84$). However, there were no significant differences in the percent remaining between sCT and Mal-sCT at 2 ($p=0.094$) and 5 ($p=0.072$) min based on the 2-tailed t-test.

Liver Metabolism

After 15 min of incubation in the liver juice, less than 1% of sCT was detected, indicating a rapid degradation of the peptide by the liver enzymes. When the incubation period was prolonged to 30 min, there was negligible amount of sCT remaining, and the peptide became undetectable after

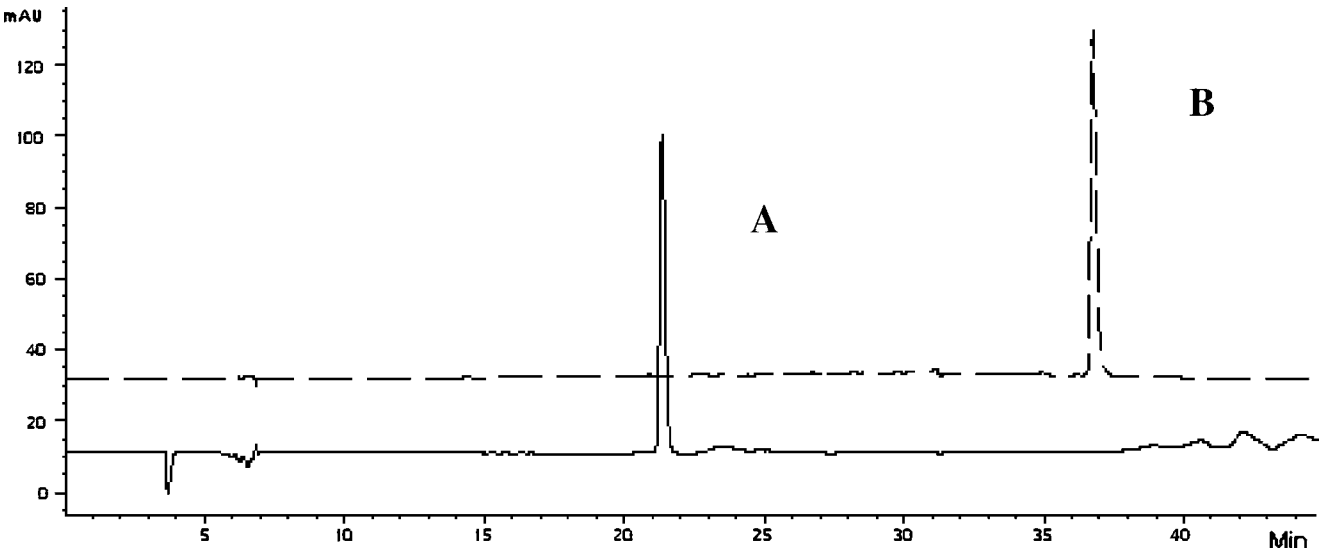

Fig. 3. HPLC chromatograph of (A) sCT and (B) Mal-sCT.

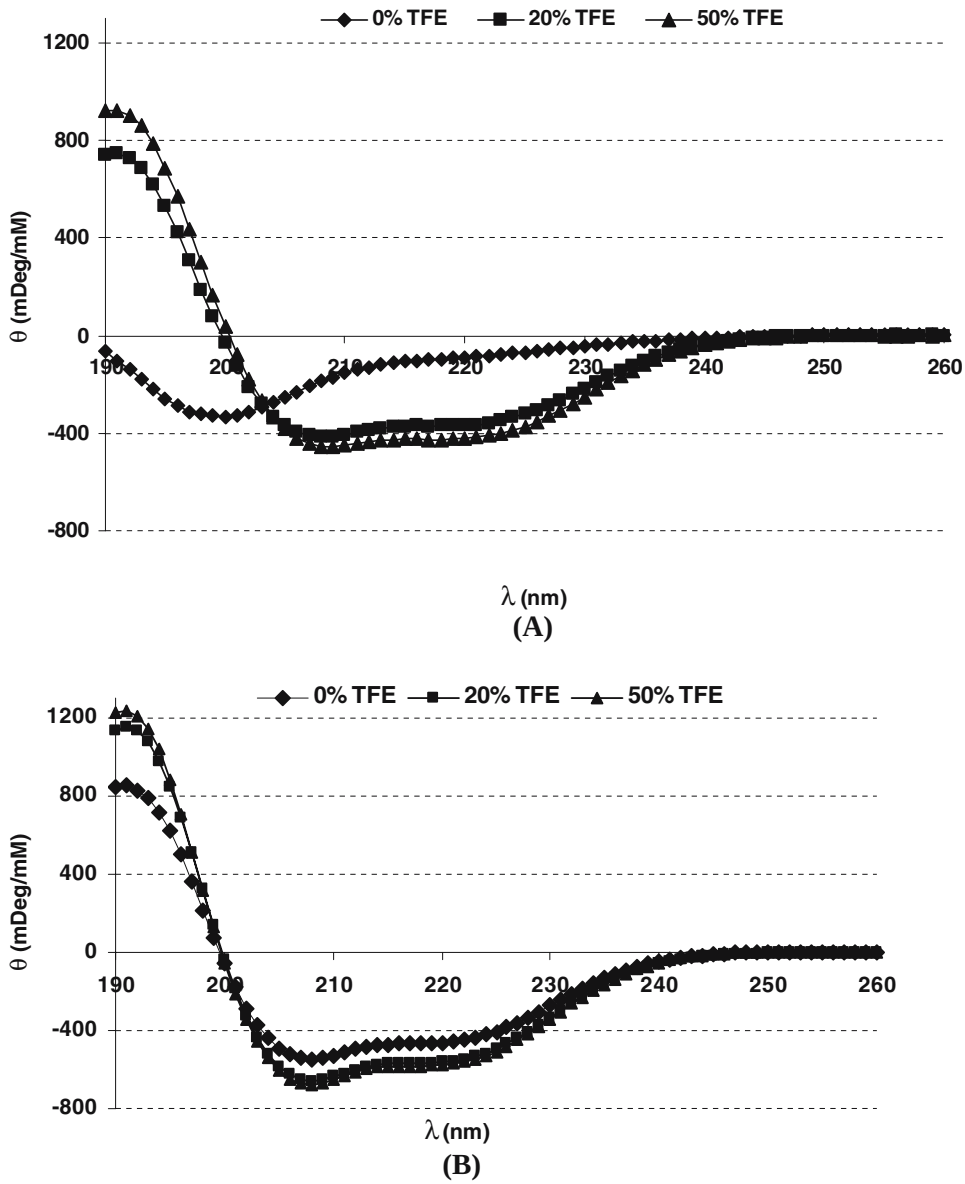

Fig. 4. Circular dichroism spectra of (A) sCT and (B) Mal-sCT in aqueous solutions containing different concentrations of trifluoroethanol (*TFE*). Peptides were analyzed at a concentration of 0.10 mM.

45 min of incubation (Fig. 7). In comparison, Mal-sCT showed a slower rate of liver metabolism, with 86.4% of the conjugate remaining after 15 min of incubation in the liver juice. Even when the incubation period was prolonged to 90 min, about 10% of the conjugate remained detectable in the juice. The degradation data for sCT and Mal-sCT fitted a first order degradation profile to give the following respective equations: $Y=100e^{-0.231X}$ ($R^2=0.91$) and $Y=100e^{-0.0195X}$ ($R^2=0.92$), where Y represents the percent remaining after incubation. A comparison of the two equations suggests that Mal-sCT was 11.8-fold more resistant than sCT against liver metabolism.

Cellular Uptake by Caco-2 Cells

Initial uptake of FITC-sCT and FITC-Mal-sCT by the Caco-2 cell monolayers was rapid, with subsequent uptake occurring at slower rates (Fig. 8). At all time points, the cellular uptake of FITC-Mal-sCT was about 2-fold higher than that of FITC-sCT. For example, at 145 min of incubation, the cell-associated FITC-sCT was equivalent to 2.08% of the initial load, while the corresponding figure for FITC-Mal-sCT was 4.21%.

Hypocalcemic Activity in the Rat Model

The *in vivo* bioactivity of Mal-sCT was evaluated by measuring its ability to lower plasma calcium levels after subcutaneous injection (Fig. 9) or intragastric gavage (Fig. 10) in the rat model. Rats dosed with the vehicle served as negative controls, while those administered with equivalent sCT dose were positive controls. Baseline plasma calcium levels were not significantly different between the rats in the control and treatment groups prior to treatment initiation.

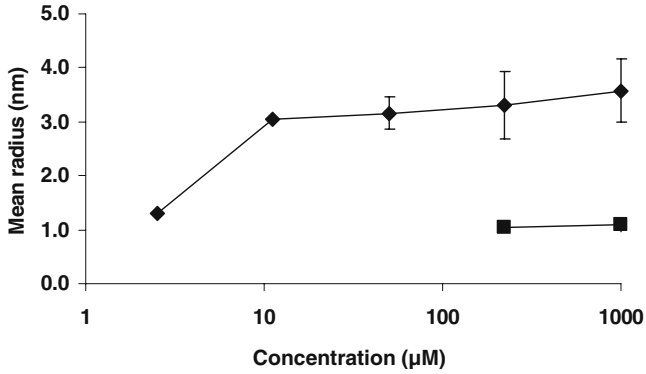

Fig. 5. Particle size as a function of concentration of sCT (*filled square*) and Mal-sCT (*filled diamond*) in water, as measured by dynamic light scattering. Data represent mean ± polydispersity of at least 20 scans.

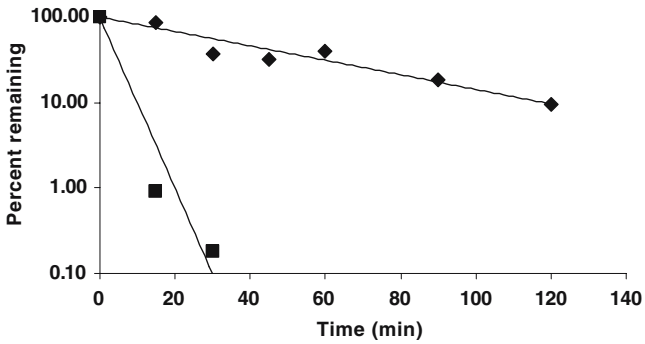

Fig. 7. Degradation profiles of sCT (*filled square*) and Mal-sCT (*filled diamond*) when incubated with fresh liver juice. Liver juice was the supernatant obtained by centrifuging a mixture of homogenized rat liver (7.5 g) and 7.5 ml of MEM (with 5% FBS) at 2,000 rpm. Curve fitting was based on first order kinetics.

Compared to the vehicle, Mal-sCT administered subcutaneously at a dose of 0.145 mg/kg (equivalent to 0.114 mg/kg sCT) was observed to cause a significant lowering of the plasma calcium level at 2 h post-injection (Fig. 9). The plasma calcium level remained at low levels from 2 to 12 h post-injection. Subcutaneous sCT at the same dose produced comparable results to Mal-sCT, causing a significant lowering of the plasma calcium levels from 1 to 12 h post-injection. However, Mal-sCT appeared to give more variable outcomes, as evidenced by the wider error bars for the plasma calcium levels at 8 and 12 h post-injection.

The biological activities of peroral sCT and Mal-sCT were also compared. All six rats given sCT (dose 5.0 mg/kg) by intragastric gavage showed significantly lower plasma calcium levels at 1 to 2 h post-administration ($p<0.001$), and a return of the calcium levels to baseline at 4 h post-administration (Fig. 10A). In contrast, the mean plasma calcium data obtained for peroral Mal-sCT were not statistically different from baseline levels. However, while consistent outcomes were observed for all the rats in the sCT group, the outcomes were not uniform across the six rats in the peroral Mal-sCT treatment group (Fig. 10B). The majority of the rats (four out of six) did not exhibit a lowering in plasma calcium level following the administration of Mal-sCT, but two rats in the group showed low calcium levels, about 6.5 mg/dl, from 2 to 12 h post-administration. This suggests that Mal-sCT might be effective in select individuals.

The pharmacodynamic responses attributed to peroral sCT and Mal-sCT was quantified by determining the AAIC. Mean AAIC for peroral sCT at 579±314 mg min/dL (n=6) was not statistically different from that for peroral Mal-sCT at 1254±1829 mg min/dL (n=6). Mean relative and absolute pharmacological BA for sCT were calculated to be 0.0069 and 0.0011%, respectively. These values were approximately 26-fold less than that reported for sCT delivered directly into the rat duodenum at a similar dose (27), suggesting that the peptide was significantly degraded in the gastric fluid. Mean relative pharmacological BA for peroral Mal-sCT was 0.015%, about 2-fold higher than that for peroral sCT. However, the accuracy of the BA value for Mal-sCT is compromised by the large variation in plasma calcium data obtained.

DISCUSSION

Lipid modification of peptides has gained prominence in recent years for improving peptide drug deliverability (2,8,21,29,30). Chemical methods for lipidization usually target the free ε-amine of lysine or the N-terminal amine.

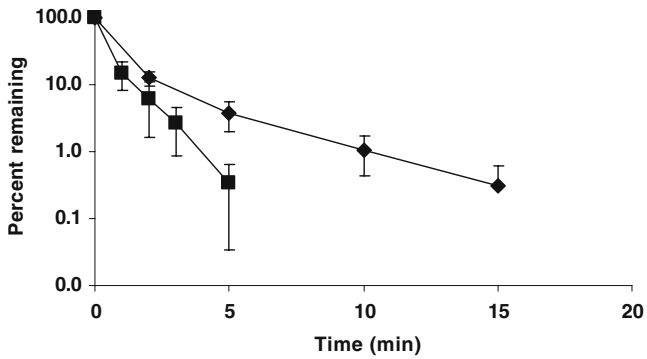

Fig. 6. Degradation profiles of sCT (*filled square*) and Mal-sCT (*filled diamond*) in intestinal solution. 40 μM of sCT and Mal-sCT were separately incubated with diluted intestinal solution (equivalent protein concentration of 45 μg/ml) at 37°C at a shaking rate of 50 rpm. Data represent mean ± SD, n=3.

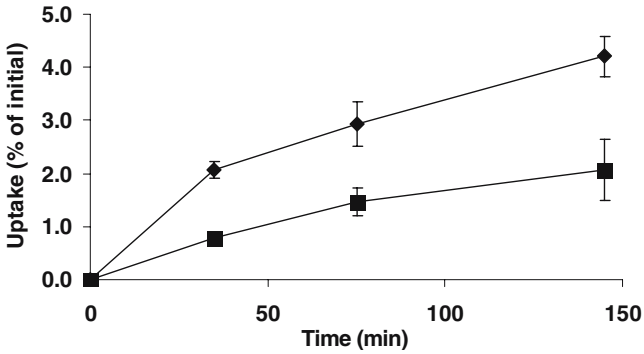

Fig. 8. Cell-associated FITC-sCT (*filled square*) and FITC-Mal-sCT (*filled diamond*) as a function of incubation time with Caco-2 cell monolayers. HBSS (pH 7.4) served as transport medium and the loading dose of peptide was 100 μl at concentration of 5.0 μM. Data represent mean ± SD, n=6.

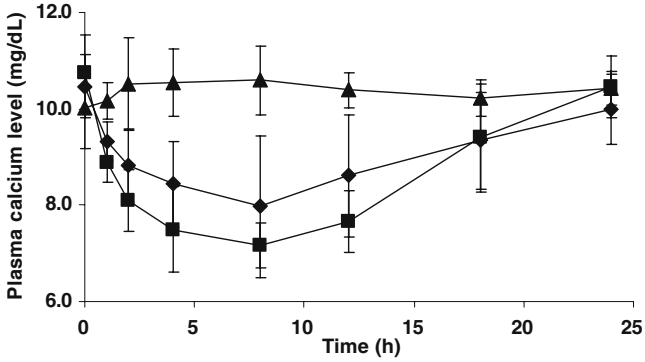

Fig. 9. Plasma calcium level of rats administered with sCT (*filled square*), Mal-sCT (*filled diamon*) and normal saline (*filled triangle*) by subcutaneous injection. sCT and Mal-sCT, dissolved in normal saline solutions at 0.114 mg/ml and 0.145 mg/ml (equivalent to 0.114 mg/ml sCT), respectively, were dosed at 200 μl/rat (200 g). Data represent mean ± SD, n=6.

These methods inevitably involved the use of noxious organic solvents, such as chloroform and dimethylformide, which are hardly favorable for maintaining peptide drug stability (31,32). In addition, solvent removal is mandatory, requiring complicated post-processing (20). On this basis, the ability to conjugate a lipid to a peptide drug in an aqueous media is highly desirable.

A water-soluble lipid, cysteine 2-pyridine disulfide derivative of palmitic acid, has previously been applied to the lipidization of protein drugs via a reversible disulfide bond (9,11). Ionization of the carboxyl group at cysteine at neutral pH significantly improved the aqueous solubility of the lipid, thereby allowing the conjugation process to be performed in an aqueous environment. The disulfide bond between the lipid and the peptide was designed to break down under reductive conditions, e.g., in the liver, to generate the peptide drug *in vivo* (11). Our hypothesis was that a non-reversible, aqueous-based lipid conjugation at the disulfide bond was also feasible, and that it would confer greater benefits in terms of presenting consistent stability to the peptide drug *in vivo*, provided the lipid modification did not compromise the activity of the peptide. To evaluate the hypothesis, salmon calcitonin, a 32-amino acid peptide drug for inhibiting bone resorption, was used as the model compound to produce the analog, Mal-sCT.

Using straightforward synthesis procedures, we have shown that Mal-sCT could be obtained at high purity and yield. More importantly, the lipid modification did not compromise the hypocalcemic activity of the peptide, thereby confirming that the disulfide moiety in sCT was not critical for its biological activity. HPLC analysis did not show the appearance of sCT when Mal-sCT was incubated with the liver juice, suggesting that the thio-ether bond in Mal-sCT was stable under reductive conditions. The implication is that the *in vivo* hypocalcemic activity of Mal-sCT could be attributed to the analog itself, not to the parent compound. At sCT equivalent dose of 0.114 mg/kg, Mal-sCT showed comparable hypocalcaemic activity to sCT following subcutaneous injection in the rat model. While this might suggest comparable bone resorption activities for the two compounds, it should be noted that the plasma calcium level has a threshold value because of homeostasis (27). Therefore, differences in bone resorption activity between two compounds, particularly at high doses, might not be reflected by significantly different plasma calcium levels (12) despite reports on a direct correlation between plasma calcium level and bone resorption activity (33,34). Further studies, e.g., the comparison of ED50 values, will have to be conducted to establish whether subcutaneously injected Mal-sCT is bioequivalent to sCT.

The CD data provided an interesting correlation of sCT activity to its conformation. sCT was shown to exhibit a highly labile conformation in an aqueous medium, changing from random coil to helical structure as the polarity of the medium was decreased (Fig. 4). By comparison, the conformation of Mal-sCT was independent of the polarity of the medium, the peptide maintaining a helical structure in aqueous media containing 0–50% of TFE. This has significant implications because the manifold conformations of sCT in aqueous solutions have not allowed its active conformation to be resolved to date (27). Mal-sCT is the first sCT analog to show a robust helical structure in aqueous solutions, and by inference of its comparable hypocalcemic activity *in vivo*, would suggest that the helical sCT is a biologically active molecule.

The dynamic light scattering data suggested that Mal-sCT formed aggregates over the concentration range of 11 to 1,000 μM in water (Fig. 5). This is not a unique phenomenon, because other lipidated peptides, e.g., insulin conjugated with

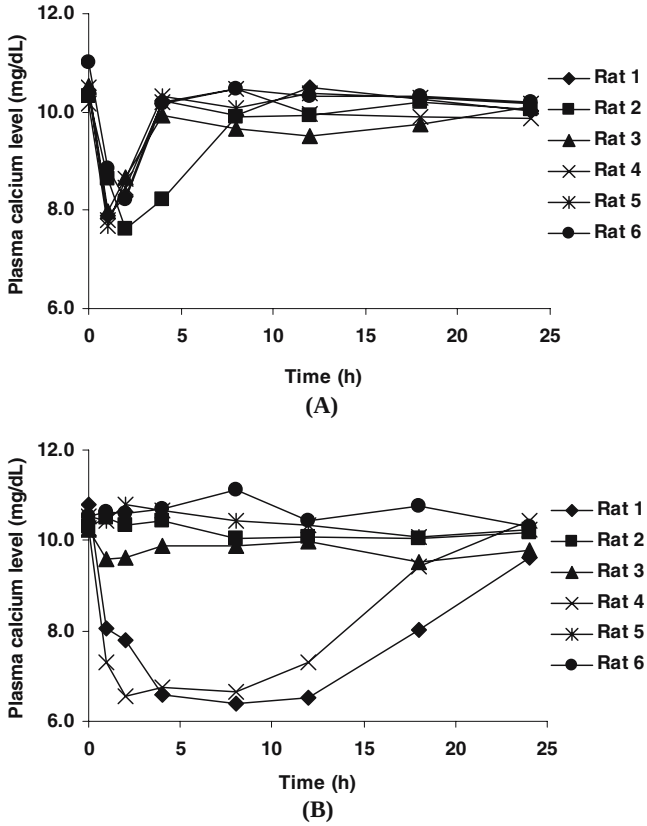

Fig. 10. Plasma calcium level of six individual rats after intragastric gavage with sCT (A) and Mal-sCT (B). sCT and Mal-sCT were administered as 2.5 mg/ml and 3.2 mg/ml (equivalent to 2.5 mg/ml sCT) solutions in water, respectively. Dose administered for sCT and Mal-sCT was equivalent to 5.0 mg/kg of sCT.

myristoyl or deoxycholic acid (21,35), have been reported to show aggregation behavior in water. Micellization of the amphiphilic Mal-sCT was likely to be promoted in water through the segregation of the dual lipid chains to form a microenvironment of low dielectric constant. The propensity of Mal-sCT to aggregate in water probably underpinned its enhanced stability in the liver juice, since the aggregates will limit enzyme access to individual Mal-sCT molecules. In contrast, sCT existed predominantly as monomers in aqueous media and it was rapidly degraded by the liver enzymes. This contradicts the findings by Sinko's group, who showed negligible hepatic first-pass elimination of sCT following portal venous injection into beagle dogs (36). The contradiction may have arise from the higher concentration of liver enzymes used in the present study.

Transformation of sCT to Mal-sCT improved its degradation against the hepatic peptidases. Although it might be argued that the enhancement in stability was not encouraging, this level was in agreement with some reports, e.g., the lipidization of desmopressin was shown to cause 11.5-fold resistance to enzyme degradation (11). On the other hand, Mal-sCT showed comparable degradation rate to sCT in the diluted intestinal fluid, suggesting that the aggregated state of Mal-sCT did not confer protection against the intestinal peptidases. This is not unusual, for the lipidization of peptide drugs does not always result in protection against enzyme degradation. In one study, the lipidization of insulin was shown to decrease the peptide stability in intestinal fluid by 1.9-fold (7). Nevertheless, the failure of Mal-sCT to resist degradation in the intestinal fluid does bring into question the practicality of synthesizing Mal-sCT. However, as the same lipidization process does not often bring about equitable enzyme stability for different peptides (7,37), it is conceivable that the novel synthetic pathway that was developed in this study may still prove useful for stabilizing other peptides to enzyme degradation.

Mal-sCT showed 2-fold stronger cellular uptake compared to sCT in the Caco-2 cell model. The stronger cellular association of Mal-sCT is not surprising given its greater lipophilicity. Cellular uptake experiments were conducted with dilute sCT and Mal-sCT solutions (5 μM) to avoid uptake saturation. At this concentration, both sCT and Mal-sCT existed as monomers. Therefore the higher cellular uptake of Mal-sCT could not be attributed to an aggregation phenomenon.

The oral BA of Mal-sCT dissolved in water was determined in the present study. Despite many publications reporting on the enhanced stability (3,4), cellular uptake (9) or both (29,37) of lipidized peptide drugs, there is little data on their *in vivo* activity. Often, the higher oral bioavailability of the peptides was alluded to based on the *in vitro* data (9,12,21,29,37), and what little *in vivo* data available on these conjugates were derived with specially designed pharmaceutical formulations (12). In view of its greater resistance to liver metabolism and stronger cellular association, Mal-sCT was anticipated to have greater oral bioavailability than sCT. This was not evident from the *in vivo* data. Mal-sCT, delivered by intragastric gavage as dissolved molecules in water at equivalent sCT dose and concentration, did not produce mean plasma calcium levels that were significantly different from the baseline level at all the time points measured. In contrast, peroral sCT solution at the same dose was observed to significantly lower the plasma calcium level of the rats to 20% at 1 h post-administration, and to maintain this level for the next 1–3 h.

Wide variation in within-group outcome was seen with peroral Mal-sCT, with four out of six rats not responding, while two rats showed a highly favorable outcome in which the plasma calcium level was reduced by up to 40% from the baseline level for a prolonged period of time of up to 10 h. Several factors may explain the variation. Firstly, the oral route of administration is known to produce significant within-group variations in BA, in particular for compounds with very low oral BA. Nonetheless, the pharmacodynamic responses for all the rats in the sCT treatment group were highly comparable. Mal-sCT, however, had a propensity to aggregate in aqueous media. If it were to aggregate into larger particles in the GIT, variable absorption profiles could result (38,39). Depending on the stability of the aggregates in the GIT, Mal-sCT could be absorbed as particulates, in which case, absorption would occur predominantly through the M cells of the Peyer's patch, a route that tends to give highly variable BA (40).

The variation in pharmacodynamic response might also result from factors other than absorption (41). This is because Mal-sCT also produced greater variability in plasma calcium levels compared to sCT when it was administered to the rats by subcutaneous injection (Fig. 9). Such pharmacological variation has not been reported for other non-reversible lipid-conjugates, such as insulin (8,21,42), indicating that the increase in lipophilicity of the molecule was not an influencing factor. Mal-sCT appeared to have a more rigid conformation in water, and this could have limited its capacity to bind with certain receptor phenotypes. Calcitonin receptors in human (43,44) and in the rat (45–48) are known to show genetic polymorphisms. The calcitonin receptor was hypothesized to bind with sCT, and its analogues, in a 2-step process that involved the peptide backbone/receptor interaction followed by the peptide side-chain/receptor interaction (45,49,50). sCT is proposed to adopt an extended conformation to participate in the first reaction, followed by a restructuring into the helical conformation for the subsequent reaction due to the decreased polarity at the membrane interface (51). Mal-sCT lacks this flexibility; its rigid helical conformation might favor the second reaction, but would hinder the peptide from making the initial interaction with the receptor. The therapeutic outcome of peroral Mal-sCT could be further complicated by the genetic polymorphisms of metabolic enzymes (52). More experiments are being planned to provide a better understanding of the behavior of Mal-sCT *in vivo*.

In conclusion, we have reported a novel method for conjugating a water-soluble lipid to sCT to generate a novel, non-reversible, water-soluble lipid-sCT conjugate at high yield. This conjugate, denoted as Mal-sCT, showed higher lipophilicity and a stable helix structure in aqueous solutions of varying degrees of polarity. Compared with sCT, the conjugate had a stronger tendency to form aggregates, was more resistant to enzyme degradation, and exhibited stronger cellular association. Biological activity was not compromised by the lipid conjugation, as Mal-sCT produced comparable hypocalcaemic activity to sCT when injected subcutaneously

into the rat model. The biological activity of peroral Mal-sCT was, however, inconclusive due to wide within-group variations in therapeutic response.

ACKNOWLEDGMENTS

This research was supported by a National University of Singapore Academic Research Fund (R148-000-045-112). Weiqiang Cheng is grateful to the National University of Singapore for financial support of his graduate studies. The authors thank Dr. J. Sivaraman (Department of Biological Sciences, NUS) for his help with the DLS experiments.

REFERENCES

1. M. Ellmerer, M. Hamilton-Wessler, S. P. Kim, M. K. Dea, E. Kirkman, A. Perianayagam, J. Markussen, and R. N. Bergman. Mechanism of action in dogs of slow-acting insulin analog O346. *J. Clin. Endocrinol. Metab.* **88**:2256–2262 (2003).
2. S. Havelund, A. Plum, U. Ribel, I. Jonassen, A. Volund, J. Markussen, and P. Kurtzhals. The mechanism of protraction of insulin detemir, a long-acting, acylated analog of human insulin. *Pharm. Res.* **21**:1498–1504 (2004).
3. J. Wang and W. C. Shen. Gastric retention and stability of lipidized Bowman–Birk protease inhibitor in mice. *Int. J. Pharm.* **204**:111–116 (2000).
4. F. Delie, P. Couvreur, D. Nisato, J. B. Michel, F. Puisieux, and Y. Letourneux. Synthesis and *in vitro* study of a diglyceride prodrug of a peptide. *Pharm. Res.* **11**:1082–1087 (1994).
5. J. Markussen, S. Havelund, P. Kurtzhals, A. S. Andersen, J. Halstrom, E. Hasselager, U. D. Larsen, U. Ribel, L. Schaffer, K. Vad, and I. Jonassen. Soluble, fatty acid acylated insulins bind to albumin and show protracted action in pigs. *Diabetologia* **39**: 281–288 (1996).
6. A. V. Kabanov, A. V. Ovcharenko, N. S. Melik-Hubarov, A. I. Bannikov, V. Alakhov, V. I. Kiselev, P. G. Sveshnikov, O. I. Kiselev, A. V. Levashov, and E. S. Severin. Fatty acid acylated antibodies against virus suppress its reproduction in cells. *FEBS Lett.* **250**:238–240 (1989).
7. H. Asada, T. Douen, Y. Mizokoshi, T. Fujita, M. Murakami, A. Yamamoto, and S. Muranishi. Stability of acyl derivatives of insulin in the small intestine: relative importance of insulin association characteristics in aqueous solution. *Pharm. Res.* **11**:1115–1120 (1994).
8. M. Hashimoto, K. Takada, Y. Kiso, and S. Muranishi. Synthesis of palmitoyl derivatives of insulin and their biological activities. *Pharm. Res.* **6**:171–176 (1989).
9. H. M. Ekrami, A. R. Kennedy, and W. C. Shen. Water-soluble fatty acid derivatives as acylating agents for reversible lipidization of polypeptides. *FEBS Lett.* **371**:283–286 (1995).
10. J. Wang, D. Shen, and W. C. Shen. Preparation, purification, and characterization of a reversibly lipidized desmopressin with potentiated anti-diuretic activity. *Pharm. Res.* **16**:1674–1679 (1999).
11. J. Wang, D. Wu, and W. C. Shen. Structure–activity relationship of reversibly lipidized peptides: studies of fatty acid–desmopres sin conjugates. *Pharm. Res.* **19**:609–614 (2002).
12. J. Wang, D. Chow, H. Heiati, and W. C. Shen. Reversible lipidization for the oral delivery of salmon calcitonin. *J. Control. Release* **88**:369–380 (2003).
13. L. Yuan, J. Wang, and W. C. Shen. Reversible lipidization prolongs the pharmacological effect, plasma duration, and liver retention of octreotide. *Pharm. Res.* **22**:220–227 (2005).
14. J. H. Cort, O. Schuck, J. Stribrna, J. Skopkova, K. Jost, and J. L. Mulder. Role of the disulfide bridge and the C-terminal tripeptide in the antidiuretic action of vasopressin in man and the rat. *Kidney Int.* **8**:292–302 (1975).
15. S. Gazal, G. Gelerman, O. Ziv, O. Karpov, P. Litman, M. Bracha, M. Afargan, and C. Gilon. Human somatostatin receptor specificity of backbone-cyclic analogues containing novel sulfur building units. *J. Med. Chem.* **45**:1665–1671 (2002).
16. M. Afargan, E. T. Janson, G. Gelerman, R. Rosenfeld, O. Ziv, O. Karpov, A. Wolf, M. Bracha, D. Shohat, G. Liapakis, C. Gilon, A. Hoffman, D. Stephensky, and K. Oberg. Novel long-acting somatostatin analog with endocrine selectivity: potent suppression of growth hormone but not of insulin. *Endocrinology* **142**:477–486 (2001).
17. R. C. Orlowski, R. M. Epand, and A. R. Stafford. Biologically potent analogues of salmon calcitonin which do not contain an N-terminal disulfide-bridged ring structure. *Eur. J. Biochem.* **162**:399–402 (1987).
18. Y. Wang, H. Dou, C. Cao, N. Zhang, J. Ma, J. Mao, and H. Wu. Solution structure and biological activity of recombinant salmon calcitonin S-sulfonated analog. *Biochem. Biophys. Res. Commun.* **306**:582–589 (2003).
19. C. Peters, A. Wolf, M. Wagner, J. Kuhlmann, and H. Waldmann. The cholesterol membrane anchor of the Hedgehog protein confers stable membrane association to lipid-modified proteins. *Proc. Natl. Acad. Sci. USA* **101**:8531–8536 (2004).
20. J. T. Elliott and G. D. Prestwich. Maleimide-functionalized lipids that anchor polypeptides to lipid bilayers and membranes. *Bioconjug. Chem.* **11**:832–841 (2000).
21. S. Lee, K. Kim, T. S. Kumar, J. Lee, S. K. Kim, D. Y. Lee, Y. K. Lee, and Y. Byun. Synthesis and biological properties of insulin-deoxycholic acid chemical conjugates. *Bioconjug. Chem.* **16**: 615–620 (2005).
22. O. Keller and J. Rudinger. Preparation and some properties of maleimido acids and maleoyl derivatives of peptides. *Helv. Chim. Acta* **58**:531–541 (1975).
23. K. Wakisaka, Y. Arano, T. Uezono, H. Akizawa, M. Ono, K. Kawai, Y. Ohomomo, M. Nakayama, and H. Saji. A novel radioiodination reagent for protein radiopharmaceuticals with L-lysine as a plasma-stable metabolizable linkage to liberate m-iodohippuric acid after lysosomal proteolysis. *J. Med. Chem.* **40**:2643–2652 (1997).
24. S. Mansoor, Y. S. Youn, and K. C. Lee. Oral delivery of mono-PEGylated sCT (Lys18) in rats: regional difference in stability and hypocalcemic effect. *Pharm. Dev. Technol.* **10**:389–396 (2005).
25. G. T. Hermanson. *Bioconjugate Techniques*, Academic, San Diego, CA, 1996.
26. Z. Ma and L. Y. Lim. Uptake of chitosan and associated insulin in Caco-2 cell monolayers: a comparison between chitosan molecules and chitosan nanoparticles. *Pharm. Res.* **20**:1812–1819 (2003).
27. P. J. Sinko, C. L. Smith, L. T. McWhorter, W. Stern, E. Wagner, and J. P. Gilligan. Utility of pharmacodynamic measures for assessing the oral bioavailability of peptides. 1. administration of recombinant salmon calcitonin in rats. *J. Pharm. Sci.***84**:13 74–1378 (1995).
28. J. C. Van Loon. *Analytical Atomic Absorption Spectroscopy: Selected Methods*, Academic, New York, 1980.
29. T. Uchiyama, A. Kotani, H. Tatsumi, T. Kishida, A. Okamoto, N. Okada, M. Murakami, T. Fujita, Y. Fujiwara, Y. Kiso, S. Muranishi, and A. Yamamoto. Development of novel lipophilic derivatives of DADLE (leucine enkephalin analogue): intestinal permeability characateristics of DADLE derivatives in rats. *Pharm. Res.* **17**:1461–1467 (2000).
30. Y. J. Tsai, A. Rottero, D. D. Chow, K. J. Hwang, V. H. Lee, G. Zhu, and K. K. Chan. Synthesis and purification of NB1-palmitoyl insulin. *J. Pharm. Sci.* **86**:1264–1268 (1997).
31. M. Sukumar, S. M. Storms, and M. R. De Felippis. Non-native intermediate conformational states of human growth hormone in the presence of organic solvents. *Pharm. Res.***22**:789–796 (2005).
32. H. Sah. Protein behavior at the water/methylene chloride interface. *J. Pharm. Sci.* **88**:1320–1325 (1999).
33. K. Nishiki, S. Tsuruoka, M. Wakaumi, H. Yamamoto, A. Koyama, and A. Fujimura. Dosing time-dependent variation in the hypocalcemic effect of calcitonin in rat. *Eur. J. Pharmacol.* **460**:171–175 (2003).
34. T. Buclin, M. Cosma Rochat, P. Burckhardt, M. Azria, and M. Attinger. Bioavailability and biological efficacy of a new oral formulation of salmon calcitonin in healthy volunteers. *J. Bone Miner. Res.* **17**:1478–1485 (2002).

35. H. B. Olsen and N. C. Kaarsholm. Structural effects of protein lipidation as revealed by LysB29-myristoyl, des(B30) insulin. *Biochemistry* **39**:11893–11900 (2000).
36. Y. Hee Lee, G. D. Leesman, V. Makhey, H. Yu, P. Hu, B. Perry, J. P. Sutyak, E. J. Wagner, L. M. Falzone, W. Stern, and P. J. Sinko. Regional oral absorption, hepatic first-pass effect, and non-linear disposition of salmon calcitonin in beagle dogs. *Eur. J. Pharm. Biopharm.* **50**:205–211 (2000).
37. E. Yodoya, K. Uemura, T. Tenma, T. Fujita, M. Murakami, A. Yamamoto, and S. Muranishi. Enhanced permeability of tetragastrin across the rat intestinal membrane and its reduced degradation by acylation with various fatty acids. *J. Pharmacol. Exp. Ther.* **271**:1509–1513 (1994).
38. H. Chen and R. Langer. Oral particulate delivery: status and future trends. *Adv. Drug Deliv. Rev.* **34**:339–350 (1998).
39. Y. V. Frenkel, A. D. Clark Jr, K. Das, Y. H. Wang, P. J. Lewi, P. A. Janssen, and E. Arnold. Concentration and pH dependent aggregation of hydrophobic drug molecules and relevance to oral bioavailability. *J. Med. Chem.* **48**:1974–1983 (2005).
40. E. C. Lavelle, S. Sharif, N. W. Thomas, J. Holland, and S. S. Davis. The importance of gastrointestinal uptake of particles in the design of oral delivery systems. *Adv. Drug Deliv. Rev.* **18**:5–22 (1995).
41. G. Levy. Impact of pharmacodynamic variability on drug delivery(1). *Adv. Drug Deliv. Rev.* **33**:201–206 (1998).
42. H. Mei, C. Yu, and K. K. Chan. NB1-C16-insulin: site-specific synthesis, purification, and biological activity. *Pharm. Res.* **16**:1680–1686 (1999).
43. I. Zofkova, K. Zajickova, and M. Hill. Postmenopausal serum androstenedione levels are associated with the calcitonin receptor gene polymorphism T1377c. A pilot study. *J. Endocrinol. Investig.* **27**:442–444 (2004).
44. V. Braga, A. Sangalli, G. Malerba, M. Mottes, S. Mirandola, D. Gatti, M. Rossini, M. Zamboni, and S. Adami. Relationship among VDR (BsmI and FokI), COLIA1, and CTR polymorphisms with bone mass, bone turnover markers, and sex hormones in men. *Calcif. Tissue Int.* **70**:457–462 (2002).
45. H. Nakamuta, R. C. Orlowski, and R. M. Epand. Evidence for calcitonin receptor heterogeneity: binding studies with non-helical analogs. *Endocrinology* **127**:163–169 (1990).
46. J. M. Hilton, S. Y. Chai, and P. M. Sexton. *In vitro* autoradiographic localization of the calcitonin receptor isoforms, C1a and C1b, in rat brain. *Neuroscience* **69**:1223–1237 (1995).
47. P. M. Sexton, S. Houssami, J. M. Hilton, L. M. O'Keeffe, R. J. Center, M. T. Gillespie, P. Darcy, and D. M. Findlay. Identification of brain isoforms of the rat calcitonin receptor. *Mol. Endocrinol.* **7**:815–821 (1993).
48. M. Ikegame, M. Rakopoulos, H. Zhou, S. Houssami, T. J. Martin, J. M. Moseley, and D. M. Findlay. Calcitonin receptor isoforms in mouse and rat osteoclasts. *J. Bone Miner. Res.* **10**: 59–65 (1995).
49. G. Siligardi, B. Samori, S. Melandri, M. Visconti, and A. F. Drake. Correlations between biological activities and conformational properties for human, salmon, eel, porcine calcitonins and Elcatonin elucidated by CD spectroscopy. *Eur. J. Biochem.* **221**: 1117–1125 (1994).
50. S. Houssami, D. M. Findlay, C. L. Brady, T. J. Martin, R. M. Epand, E. E. Moore, E. Murayama, T. Tamura, R. C. Orlowski, and P. M. Sexton. Divergent structural requirements exist for calcitonin receptor binding specificity and adenylate cyclase activation. *Mol. Pharmacol.* **47**:798–809 (1995).
51. A. Motta, A. Pastore, N. A. Goud, and M. A. Castiglione Morelli. Solution conformation of salmon calcitonin in sodium dodecyl sulfate micelles as determined by two-dimensional NMR and distance geometry calculations. *Biochemistry* **30**:10444–10450 (1991).
52. M. O. Goodarzi, K. D. Taylor, X. Guo, M. J. Quinones, J. Cui, X. Li, T. Hang, H. Yang, E. Holmes, W. A. Hsueh, J. Olefsky, and J. I. Rotter. Variation in the gene for muscle-specific AMP deaminase is associated with insulin clearance, a highly heritable trait. *Diabetes* **54**:1222–1227 (2005).